# Understanding the Coupled Swing Equation

BHAIRAVI PREMNATH, ANASTASIA SOFRONIOU
School of Computing and Engineering
University of West London
St. Mary's Road, W5 5RF
UNITED KINGDOM

*Abstract:* Influenced by the nonlinear dynamics of mathematical models found in power systems, an analysis of the dynamical behaviour of the coupled swing equation is performed. The coupled formulation explains the interactions between interconnected synchronous machines, which play a critical role in modern power systems. This paper examines analytically and numerically the emergence and evolution of oscillatory periodic solutions under primary resonance. As the control parameter is altered, the system undergoes a cascade of period-doubling bifurcations, which leads to loss of stability and the onset of complex dynamical behaviour can be observed. Phase portraits, time series and Poincaré maps are used to characterise the transition between different dynamical patterns to identify the precursors to instability. A thorough understanding of the system's behaviour shows valuable insights into bifurcation with the appearance of the initial period doubling phenomena, depicting early indicators of adverse effects that can occur within an interconnected power system.

*Key-Words:* nonlinear dynamics; power system; swing equation; coupling; bifurcation; chaos.

Received: April 29, 2025. Revised: December 15, 2025. Accepted: March 8, 2025. Published: June 3, 2026.

## 1 Introduction

The stability of a power system fundamentally depends on the response to disturbances that can occur when sudden or sequential changes happen within system parameters, different operating states or loading conditions, [1], [2]. Even a minute disturbance can cause complex dynamical behaviour, specifically in interconnected systems where interactions are present between multiple machines. Standard stability analysis techniques depend solely on linearising the governing equations and applying frequency response methods or eigenvalue calculations to assess system behaviour closer to the equilibrium point, [3]. While such strategies are influential for small-signal analysis, they are unable to capture the full range of nonlinear phenomena that may appear in coupled power system models.

The swing equation, a second-order differential equation, provides a comprehensive mathematical description of both the electrical and mechanical dynamics of synchronous machines, [4]. Considering interconnected power systems, the dynamical behaviour of individual machines is not independent, but determined by their mutual interactions via the transmission network, [5]. These exchanges are generally represented through coupled swing equations, which in turn introduce extra degrees of freedom and strong nonlinearities within the system analysed. Due to this, coupled swing equations can exhibit rich dynamical behaviour such as synchronisation, bifurcation, resonance and instability, which are less seen in single-machine systems, [6].

Recently, the complexity of modern power systems has increased rapidly, particularly due to higher levels of interconnections and integration of renewable energy sources, [7], [8]. This has encouraged researchers to study and understand nonlinear dynamic effects in systems. Hence, coupled swing equations offer a simplified yet powerful framework to investigate multiple machine behaviours under different external and parametric excitations, [9]. When two busbars are connected and stability is analysed, it is important to consider the coupling between the two machines to thoroughly understand the stability. This paper studies the dynamical behaviour of the coupled swing equation using both analytical and numerical methods. It emphasises the importance of identifying oscillatory solutions and examining how changes in key parameters impact the stability of the system. The analysis also focuses on the bifurcation of the coupled swing equation, with specific attention drawn to period doubling phenomena and their influence as precursors to instability. Phase portraits, time-series diagrams and Poincaré maps are employed to understand the system response and provide insights into the nonlinear mechanisms governing the dynamics of the swing equation.

### 1.1 Brief Literature Review

A power system is in a stable state at a given condition if it can maintain synchronism and return to a steady state following a disturbance in the system, [10]. For very small disturbances, linearised systems are generally enough to discuss the dynamical behaviour, [11]. But, when the disturbances are strong or large, nonlinear exchanges are present and linear approximations become inadequate, hence numerical simulations and nonlinear analysis are used, [12]. The swing equation has been used for a very long time to model the synchronous dynamics of the system and study oscillatory and transient stability. Previous studies primarily focused on single machine representations linked to an infinite busbar system, which provided important insights into the fundamental stability of the model, [1], [13]. However, they do not discuss enough about the impact of machine-to-machine interactions that are essential in interconnected power systems. To address this, authors have extended the swing equation to a coupled model that explicitly accounts for mutual coupling effects.

A model with coupled swing equations has been shown to exhibit a wide range of nonlinear behaviours, including resonance and complex oscillatory motion, [14]. Various analytical strategies like perturbation methods, averaging techniques and bifurcation theory have been applied to study these phenomena, [13]. Numerical approaches and geometric tools like phase portraits and Poincaré maps have been particularly effective in showing qualitative changes in the dynamics of the systems that are not seen by linear analysis, [15].

Bifurcation analysis plays an important role in understanding how small variations in system parameters can cause significant qualitative changes in the system's dynamical behaviour, [16]. In power system models, bifurcations are closely connected with critical points such as oscillatory instability and loss of synchronism, [17]. But the particular interest falls on the period-doubling bifurcation, which often acts as an early indicator for instability and can lead up to the onset of chaotic dynamics, [18].

External and parametric excitations play a vital role in influencing the dynamic response of the swing equation system. When the frequency of an external excitation is approximately equal to the natural frequency of the system is called the primary resonance and may occur, which can result in large amplitude oscillations and increase sensitivity to parameter alterations, [1]. Considering the dynamics of the swing equation, primary resonance has been shown to highly impact stability boundaries, [13]. The presence of coupling further alters the behaviour of the resonance by incorporating additional interactions and hence improving the overall dynamical response of the model.

Recent literature has emphasised the importance of identifying the precursors to chaos to improve system monitoring and operational decision-making, [19]. Influenced by these results, the present work focuses on the coupled swing equation and aims to provide a thorough understanding of its nonlinear behaviour and primary resonance within this system. By both numerical simulations and analytical insights, this paper seeks to contribute to a deeper comprehension of the underlying mechanisms of stability within interconnected power systems.

## 2 Methodology

This study investigates the effects of coupling on the classical swing equation system, focusing on analytical and numerical techniques for primary resonance. The swing equation considered in this study is given below, [1], [13], [20]:

$$\frac{2H}{\omega_R}\frac{d^2\theta}{dt^2} + D\frac{d\theta}{dt} = P_m - \frac{V_G V_B}{X_G}\sin\left(\theta - \theta_B\right), \quad (1)$$

where the busbar voltage magnitude and phase are assumed to vary periodically as

$$V_B = V_{B0} + V_{B1}\cos\left(\Omega t + \phi_v\right), \quad (2)$$

$$\theta_B = \theta_{B0} + \theta_{B1}\cos\left(\Omega t + \phi_0\right). \quad (3)$$

with
$\omega_R$ = Constant angular velocity,
H= Inertia,
D= Damping,
$P_m$= Mechanical Power,
$V_G$= Voltage of machine,
$X_G$ = Transient Reactance,
$V_B$= Voltage of busbar system,
$\theta_B$ = phase of busbar system,

$V_{B1}$ and $\theta_{B1}$ magnitudes are assumed to be small.

### 2.1 Formulation of the Coupled Swing Equation

To account for interactions between machines, the classical swing equation is extended to a coupled formulation. For a two-machine system connected through a common busbar, the governing equations may be written as depicted below:

$$\frac{2H_1}{\omega_R}\ddot{\theta}_1 + D_1\dot{\theta}_1 = P_{m1} - P_{1B}\sin(\theta_1 - \theta_B) - K\sin(\theta_1 - \theta_2), \tag{4}$$

$$\frac{2H_2}{\omega_R}\ddot{\theta}_2 + D_2\dot{\theta}_2 = P_{m2} - P_{2B}\sin(\theta_2 - \theta_B) + K\sin(\theta_1 - \theta_2), \tag{5}$$

where $K$ denotes the coupling coefficient representing the electrical exchanges between the machines. This coupled formulation enables the study relative dynamics that arise due to machine-to-machine interactions, [21], [22].

Here, $P_{m1}$ and $P_{m2}$ represent the mechanical input powers applied to machines 1 and 2, respectively, while the electrical power output depends on the voltages, reactance and rotor angle differences. This study also focuses on the effect of primary resonance on the nonlinear behaviour of a coupled system as previously shown, [23], [24].

## 2.2 Relative-Mode Representation

For analytical coherence and to focus primarily on synchronisation dynamics, the system is expressed in relative coordinates defined by [22]:

$$\Phi = \theta_1 - \theta_2, \qquad s = \dot{\theta}_1 - \dot{\theta}_2. \tag{6}$$

Here, $\Phi$ represents the relative rotor angle between the two machines, $s$ denotes the relative angular speed.

Under the assumption of identical machines and symmetric operating conditions ($H_1 = H_2 = H$, $D_1 = D_2 = D$, $P_{m1} = P_{m2}$), the centre-of-inertia motion decouples from the internal dynamics, [23], [25], [26], yielding the relative swing equations shown below:

$$\dot{\Phi} = s, \tag{7}$$

$$\dot{s} = -\frac{D}{M}s - \frac{2K}{M}\sin\Phi, \tag{8}$$

where $M = 2H/\omega_R$. The reduced system in equations (7) and (8) governs the internal oscillatory behaviour of the coupled machines and forms the basis for the phase portraits, time-series figures and Poincaré maps shown in this study.

## 2.3 Jacobian Analysis and Local Stability

Local stability of the relative-mode dynamics is examined by linearising equations (7) and (8) about an equilibrium point $(\Phi_e, 0)$. The equilibrium conditions are given by:

$$s = 0, \qquad \sin\Phi = 0, \tag{9}$$

which yields equilibrium angles $\Phi_e = 0, \pi, \ldots$.

The Jacobian matrix of the relative system evaluated at the equilibrium point $(\Phi_e, 0)$ is:

$$J_{\text{rel}} = \begin{bmatrix} 0 & 1 \\ -\dfrac{2K}{M}\cos\Phi_e & -\dfrac{D}{M} \end{bmatrix}. \tag{10}$$

The eigenvalues of $J_{\text{rel}}$ determine the local stability characteristics of the equilibrium points. For $\Phi_e = 0$, corresponding to in-phase synchronisation, $\cos\Phi_e > 0$ and the equilibrium is locally asymptotically stable in the presence of damping. In contrast, $\Phi_e = \pi$ yields $\cos\Phi_e < 0$, resulting in a saddle-type instability. These analytical results are consistent with the phase space figures observed in the numerical simulations.

The natural frequency of small oscillations associated with the relative mode is given by:

$$\omega_{\text{rel}} = \sqrt{\frac{2K}{M}}, \tag{11}$$

and primary resonance is expected to occur when the excitation frequency $\Omega$ approaches $\omega_{\text{rel}}$. This resonance condition provides analytical justification for the observed amplification of oscillatory responses and the bifurcation behaviour identified through numerical analysis.

## 2.4 Method of Multiple Scales

To analytically study the primary resonance observed in the numerical simulations of the coupled swing equation, a weakly nonlinear approximation of the relative-mode dynamics is considered. Focusing on small oscillations about the in phase equilibrium $\Phi = 0$, the nonlinear coupling term is expanded as

$$\sin\Phi = \Phi - \frac{\Phi^3}{6} + \mathcal{O}(\Phi^5). \tag{12}$$

The periodic busbar voltage and phase variations in equation (2) and equation (3) induce a weak harmonic excitation in the relative-mode dynamics. Retaining the leading nonlinear term and incorporating this effective forcing yields the Duffing-type approximation

$$\ddot{\Phi} + \frac{D}{M}\dot{\Phi} + \omega_{\mathrm{rel}}^2\Phi - \frac{\omega_{\mathrm{rel}}^2}{6}\Phi^3 = \varepsilon F\cos(\Omega t), \quad (13)$$

where $\omega_{\mathrm{rel}}$ is given by equation (11), $\varepsilon \ll 1$ is a book keeping parameter denoting weak excitation and $F$ represents the effective forcing amplitude.

**Near-resonant scaling**

Primary resonance occurs when the excitation frequency $\Omega$ is close to $\omega_{\mathrm{rel}}$. Accordingly, the detuning is defined as

$$\Omega = \omega_{\mathrm{rel}} + \varepsilon\sigma, \quad (14)$$

where $\sigma$ is the detuning parameter. Weak damping is also assumed of order $\varepsilon$:

$$\frac{D}{M} = 2\varepsilon\mu, \quad (15)$$

with $\mu > 0$.

**Multiple-scales expansion**

Two time scales are introduced:

$$T_0 = t, \qquad T_1 = \varepsilon t.$$

A uniformly valid solution is sought in the form

$$\Phi(t;\varepsilon) = A(T_1)e^{i\omega_{\mathrm{rel}}T_0} + \overline{A(T_1)}e^{-i\omega_{\mathrm{rel}}T_0} + \mathcal{O}(\varepsilon), \quad (16)$$

where $A(T_1)$ is a slowly varying complex amplitude. Substituting equation (16) into equation (13) and eliminating secular terms at $\mathcal{O}(\varepsilon)$ yields the modulation equation

$$\frac{dA}{dT_1} = -\mu A + i\frac{\omega_{\mathrm{rel}}}{4}|A|^2A - i\frac{F}{4\omega_{\mathrm{rel}}}e^{i\sigma T_1}. \quad (17)$$

**Amplitude–phase equations**

Expressing the complex amplitude as

$$A(T_1) = \frac{1}{2}a(T_1)e^{i\beta(T_1)},$$

and defining the phase mismatch $\gamma = \sigma T_1 - \beta$, the slow-flow equations governing primary resonance are obtained:

$$\frac{da}{dT_1} = -\mu a + \frac{F}{2\omega_{\mathrm{rel}}}\sin\gamma, \quad (18)$$

$$\frac{d\gamma}{dT_1} = \sigma - \frac{\omega_{\mathrm{rel}}}{8}a^2 - \frac{F}{2\omega_{\mathrm{rel}}a}\cos\gamma. \quad (19)$$

**Steady-state response**

In steady-state primary resonance, $da/dT_1 = d\gamma/dT_1 = 0$, leading to the amplitude–frequency response equation

$$\left[\mu^2 + \left(\sigma - \frac{\omega_{\mathrm{rel}}}{8}a^2\right)^2\right]a^2 = \left(\frac{F}{2\omega_{\mathrm{rel}}}\right)^2. \quad (20)$$

Equation (20) predicts a nonlinear resonance curve with softening behaviour, explaining the strong sensitivity and amplitude amplification observed numerically when the excitation frequency is slightly detuned below $\omega_{\mathrm{rel}}$.

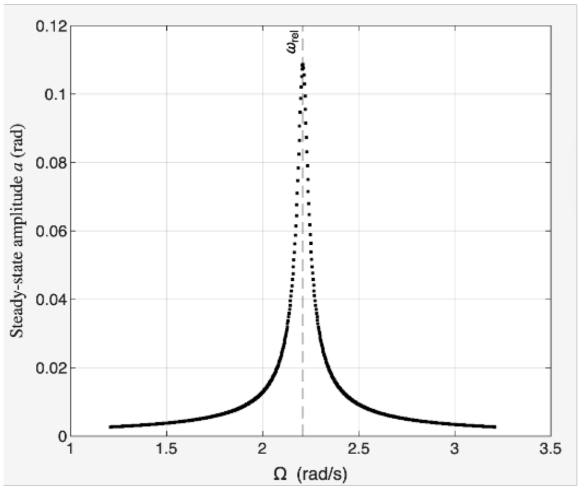


Fig. 1: Steady-state amplitude-frequency response for primary resonance. (Source: Created by the authors)

Figure 1 shows the steady-state response for the primary response predicted by equation (20). This was obtained by solving the algebraic amplitude-frequency relation for the real positive amplitude oscillation $a$ over excitation frequencies $\Omega$ near $\omega_{\mathrm{rel}}$. The curve shown above is nonlinear and may depict multiple amplitudes for a fixed $\Omega$, similar to the existing periodic responses. Since the cubic term in equation (13) is softening, the resonance peak bends toward lower frequencies, suggesting that large amplitude oscillations can occur for $\Omega < \omega_{\mathrm{rel}}$. This analytical result is consistent with the numerical results shown below in this study, where qualitative changes and amplifications in phase portraits are seen as $\Omega$ is decreased slightly below the primary resonance frequency

## 3 Results

This segment presents the outcomes of numerical simulations performed on the coupled swing equation system under primary resonance when $\Omega = 8.6$ rad/sec. All simulations were done using identical initial conditions $\Phi(0) = 0.05$ rad and $s(0) = 0$ were chosen to emphasise a small perturbation from the synchronous aspect on Matlab. Additional simulations with nearby initial conditions produced identical findings, depicting the robustness of the observed dynamical behaviour.

The equation (4) and equation (5) were configured and solved using the fourth-order Runge-Kutta method in Matlab, focusing on the effect of varying the excitation frequency $\Omega$ slightly from the primary resonance within the coupled swing equation formulation.

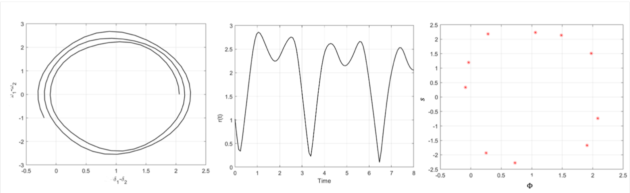

Fig. 2: Phase portrait, frequency-domain plot and Poincaré map when $\Omega = 8.58$ rad/sec. (Source: Created by the authors)

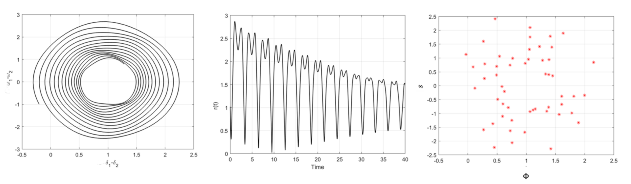

Fig. 3: Phase portrait, frequency-domain plot and Poincaré map when $\Omega = 8.4$ rad/sec. (Source: Created by the authors)

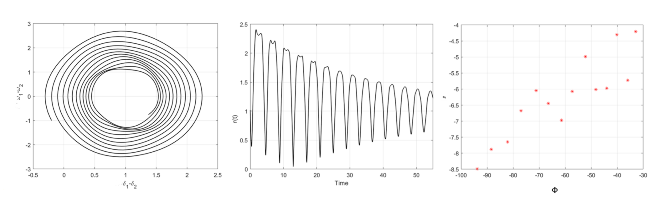

Fig. 4: Phase portrait, frequency-domain plot and Poincaré map when $\Omega = 8.278$ rad/sec. (Source: Created by the authors)

Figure 2, Figure 3, Figure 4, Figure 5 and Figure 6 were obtained by plotting the

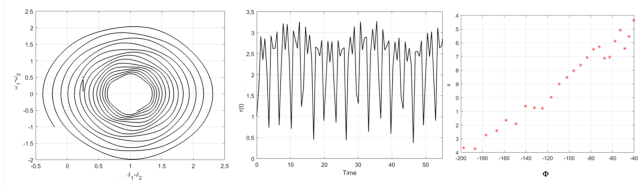

Fig. 5: Phase portrait, frequency-domain plot and Poincaré map when $\Omega = 8.269$ rad/sec. (Source: Created by the authors)

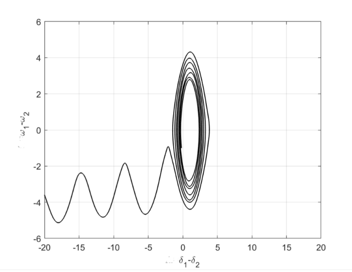

Fig. 6: Phase portrait (loss of synchronism) when $\Omega = 8.258$ rad/sec. (Source: Created by the authors)

phase portraits, time-series plots and Poincaré maps when this excitation frequency is varied in the coupled swing equation model. All phase portraits have identical axis scales to allow direct comparison. When the excitation frequency of the system of the relative mode is slightly reduced to $\Omega = 8.58$ rad/sec, closer to the primary resonance value when $\Omega = 8.6$ rad/sec, it shows a stable periodic response with spiralling orbits in the relative phase plane as shown in Figure 2. As the excitation frequency is further reduced, qualitative changes can be seen with trajectories expanding, showing an unstable equilibrium.

Figure 5 shows the phase portrait with clear difference from a simple closed orbit, while the Poincaré map shows multiple discrete points in contrast to a single fixed point. This structure is indicates higher-periodic oscillations and reflects the system's progression toward a period-doubling regime.ya

When $\Omega = 8.258$ rad/sec, Figure 6 shows loss of synchronisation and breakdown of periodic oscillatory motion. These figures emphasise the sensitivity of the coupled swing equation system to the detuning from resonance and underline the role of excitation frequency in understanding stability.

The bifurcation diagram presented as Figure 7, was constructed by solving the swing equation for a specific value of $\Omega = 8.27$ rad/sec and by numerical time integration using the classical fourth order Runge-Kutta algorithm. The forcing $r$ value is incremented slightly and time integration continues plotting the maximum amplitude of the oscillatory solution versus $r$,

$$r = \frac{V_G V_B}{X_G} \sin(\theta - \theta_B).$$

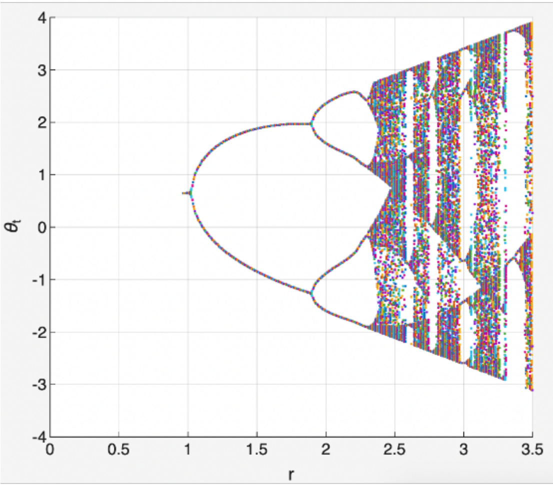


Fig. 7: Bifurcation diagram when r value is varied and constant $\Omega = 8.27$ rad/sec. (Source: Created by the authors)

Figure 7 indicates the initial period doubling occurrence just before $r = 1$ and at around $r$ approximately 2.34, the first period doubling in a sequence of period doubles is exhibited leading to chaotic behaviour. This numerical analysis shows that the swing equation moves towards loss of synchronisation as the value of $r$ is increased. The parameter $r$ was incremented using a step size of 0.005, with finer resolution near the transition area to accurately express the onset of period-doubling.

Figure 8 depicts the largest Lyapunov Exponent exhibited by the system studied, as the control parameter $r$ is varied. When $r < 2.34$ , the exponent value remains negative, showing the convergence of nearby trajectories, which therefore shows a stable periodic response. As $r$ is increased beyond the value of 2.34, the Lyapunov exponent becomes positive, showing divergence of the trajectories and the beginning of chaotic dynamics. The transformation to positive values is validated by the bifurcation diagram in Figure 6.

The numerical integration was performed using a fourth-order Runge-Kutta method with fixed step size h = 0.001. Convergence was validated by halving the step size with no qualitative changes

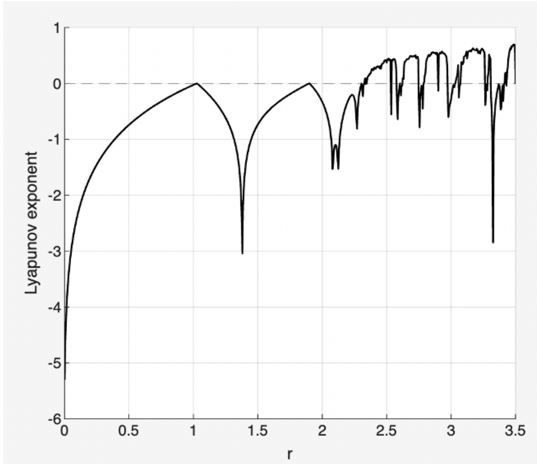


Fig. 8: Lyapunov exponents as r is varied. (Source: Created by the authors)

in the phase portraits, Lyapunov Exponents and bifurcation diagrams. The spiralling orbits shown in the above figures arise from physical damping included in the system model ($D \neq 0$) and not numerical dissipations, as verified by the convergence tests with reduced time steps.

Considering the swing equation without coupling, it exhibits simpler dynamical behaviour primarily reflecting the response to a single synchronous machine, [1], [13]. The stability also arises solely from local resonance effects. By contrast, the coupled swing equation in this study has an additional interaction term that significantly changes the nonlinear behaviour. Coupling modifies the structure of the bifurcation, which then leads to an earlier cascade to complex behaviour and also increased sensitivity to parameter variations.

Table 1: Comparison of Dynamical Behaviour: Uncoupled and Coupled Swing Equations. (Source: Created by the authors)

| **Metric** | **Uncoupled** | **Coupled** |
|---|---|---|
| Primary Resonance Response | Moderate | Strong amplification |
| Lyapunov Exponent Sign | Positive for $r > 2.4$ | Positive for $r > 2.34$ |
| Phase Space Structure | Closed orbits | Spiral orbits |
| Synchronisation Behaviour | Breaks at $\Omega = 8.2601$ rad/sec. | Breaks at $\Omega = 8.258$ rad/sec. |

Table 1 compares the dynamical behaviour of the uncoupled and coupled swing equation models under primary resonance. The uncoupled system exhibits a moderate response to primary resonance, whereas the inclusion of coupling leads to stronger amplitude amplification. This increased sensitivity is further reflected in the Lyapunov exponent behaviour, where chaotic dynamics emerge early at a slightly lower control parameter value in the coupled case ($r > 2.34$) compared to the uncoupled system ($r > 2.4$). Differences are also evident in the phase space structure, the uncoupled model maintains closed orbits indicative of periodic motion, while the coupled system displays spiral trajectories associated with loss of stability, [13]. Finally, synchronisation is observed to break at a marginally higher excitation frequency in the uncoupled model ($\Omega = 8.2601$ rad/sec) than in the coupled model ($\Omega = 8.258$ rad/sec), highlighting the destabilising influence of coupling near primary resonance.

# 4 Discussion

The results presented in this paper demonstrate dynamical behaviour arising from the coupling of swing equations under periodic excitation. The analysis is conducted in the relative state space $(\Delta, \Omega)$, which isolates the synchronisation mechanism between machines and provides a clear framework for interpreting primary resonance and stability.

The phase portraits depict that closer approximate values of excitation frequency to the primary resonance exhibit bounded oscillatory motion around the stable equilibrium point. In this context, trajectories form closed or weakly spiralling orbits showing stable periodic responses governed by the relative-mode dynamics. These findings are similar to the Jacobian analysis, which predicts local asymptotic stability when the relative angle equilibrium is satisfied.

As the excitation frequency is reduced further, a pronounced amplification of oscillatory motion can be seen. This condition of primary resonance leads to an increase in amplitude of the relative angle oscillations, which can be seen in the time-series plots. Phase portraits depict trajectories that expand and deform, reflecting the nonlinear impact of the sinusoidal coupling term. The appearance of large amplitude oscillations emphasises the sensitivity of the coupled model to resonant excitation and highlights the importance of coupling strength in shaping the dynamics of the system.

The Poincaré maps give further understanding of the qualitative change in the system behaviour. As the system parameters are varied, fixed points seen in the maps undergo bifurcation, giving rise to more discrete points within the maps. These transitions correspond to period doubling bifurcations, which indicate the onset of the increase of complex dynamical behaviour.

The bifurcation diagram also validated the occurrence of a cascade of period-doubling events as the control parameter $r$ is increased. This behaviour is characteristic of nonlinear oscillatory systems and is also an indicator of instability in the system. In the coupled swing equation, the emergence of the first period doubling bifurcation acts as an early indicator of deteriorating dynamic performance. Beyond this, the model exhibits irregular responses with structure becoming increasingly fragmented, suggesting the system is entering chaos.

Hence, the phase portraits, time-series, Poincaré maps and bifurcation diagram gives a thorough understanding of the nonlinear dynamics of the coupled swing equation. The findings demonstrate that coupling not only modifies stability boundaries but also shows different dynamic regimes that were not seen in single-machine models. These results highlight the importance of analysing relative-mode dynamics when analysing the stability of interconnected power systems.

From a real-world perspective, coupling is unavoidable in power systems as large generators are interconnected through transmission networks. The findings show that coupling fundamentally changes the system's dynamic response, impacting stability and nonlinear behaviour. Hence, it should be accounted for when analysing the resilience of modern power systems subject to even small disturbances.

# 5 Conclusion

This study has discussed an analytical and numerical investigation into the coupled swing equation's dynamical behaviour, which focused mainly on the primary resonance of the model. By improving the classical swing equation to include coupling effects and periodic excitation, a reduced relative-mode formulation was formulated, which paved the way for a clear interpretation of synchronisation and oscillatory behaviour of the system.

The Jacobian analysis established the conditions under which synchronisation remains at a stable state. Numerical simulations validated these analytical insights and demonstrated nonlinear behaviours when the parameters were altered. Mainly, the onset of primary resonance was shown to amplify oscillatory responses, which in turn lead to qualitative changes in phase space.

The appearance of period doubling bifurcation was identified as a vital mechanism driving the transition from simple periodic motion to complex behaviour. The occurrence of first-period doubling shows the early stages of dynamic degradation. Such an instance is of practical relevance as it may signal operating conditions that are highly difficult to control in real-world power systems.

In conclusion, the findings emphasise the critical role of primary resonance within the framework of the coupled swing equation in shaping nonlinear dynamics. The relative-mode adaptation in this study offers an important tool for analysing interconnected systems and provides a foundation for further research involving larger networks, parameter variations and more influence of real-world factors. The insights from this work contribute towards a deeper understanding of stability in modern world power systems.

# 6 Limitations

Although this research provides valuable insights into theoretical point of view rather than the predictive validation of the coupled swing equation model under the primary resonance, there are some limitations. The analysis is on the reduced two-machine model with symmetric parameters, which does not fully capture the network complexity of large-scale power systems. Also, the coupling between machines is modelled using a simplified sinusoidal interaction, neglecting higher-order network impacts and mechanisms that may influence real world systems. These simplifications, although necessary to focus on the fundamental behaviour, limit the applicability of the results to practical power systems and encourage further analysis using real-world scenarios.

The current study focuses on a reduced-order analytical model (relative-mode) aimed at analysing fundamental nonlinear mechanisms rather than considering industrial-related scenarios. While high-fidelity simulations and experimental validations are necessary for the practical aspect, previous studies have shown that simplified versions of the sinusoidal coupling systems express the qualitative dynamics of synchronisation, resonance and unstable points in interconnected models, [2], [13].

*References:*

[1] Sofroniou, Anastasia, Bhairavi Premnath, and Kevin Jagadissen Munisami. "An Insight into the Dynamical Behaviour of the Swing Equation." WSEAS Transactions on Mathematics 22 2023: 70-78. https://doi.org/10.37394/23206.2023.22.9.

[2] Nayfeh, M. A., Hamdan, A. M. A., and Nayfeh, A. H. Chaos and instability in a power system — Primary resonant case. Nonlinear Dynamics, 1(4), 1990 313–339. https://doi.org/10.1007/bf01865278.

[3] B. Premnath and A. Sofroniou, "Analysing Load Shedding to Increase Stability in the Swing Equation," Mathematics, vol. 13, no. 8, p. 1314, Apr. 2025, https://doi.org/10.3390/math13081314.

[4] Jun Zhou and Y. Ohsawa, "Improved Swing Equation and Its Properties in Synchronous Generators," IEEE Transactions on Circuits and Systems I: Regular Papers, vol. 56, no. 1, pp. 200–209, Jan. 2009, https://doi.org/10.1109/tcsi.2008.924895.

[5] H. M. Moussa and Y. Yu, "Dynamic Interaction of Multi-Machine Power System and Excitation Control," IEEE Transactions on Power Apparatus and Systems, vol. PAS-93, no. 4, pp. 1150–1158, Jul. 1974, https://doi.org/10.1109/tpas.1974.294061.

[6] W. Ji and V. Venkatasubramanian, "Hard-limit induced chaos in a fundamental power system model," International Journal of Electrical Power & amp; Energy Systems, vol. 18, no. 5, pp. 279–295, Jun. 1996, https://doi.org/10.1016/0142-0615(95)00066-6.

[7] X. Liang, "Emerging Power Quality Challenges Due to Integration of Renewable Energy Sources," IEEE Transactions on Industry Applications, vol. 53, no. 2, pp. 855–866, Mar. 2017, https://doi.org/10.1109/tia.2016.2626253.

[8] M. B. Prasad, P. Ganesh, K. Vinay Kumar, P. A. Mohanarao, A. Swathi, and V. Manoj, "Renewable Energy Integration in Modern Power Systems: Challenges and Opportunities," E3S Web of Conferences, vol. 591, p. 03002, 2024, https://doi.org/10.1051/e3sconf/202459103002.

[9] S. Ganesan and C. Padmanabhan, "Modelling of parametric excitation of a flexible coupling–rotor system due to misalignment," Proceedings of the Institution of Mechanical Engineers, Part C: Journal

of Mechanical Engineering Science, vol. 225, no. 12, pp. 2907–2918, Sep. 2011, https://doi.org/10.1177/0954406211411549.

[10] P. Kundur, "Power System Stability," Power System Stability and Control, May 2007, https://doi.org/10.1201/9781420009248.sec2.

[11] J. Glover and F. Schweppe, "Control of linear dynamic systems with set constrained disturbances," IEEE Transactions on Automatic Control, vol. 16, no. 5, pp. 411–423, Oct. 1971, https://doi.org/10.1109/tac.1971.1099781.

[12] A. ONEILL and V. POPE, "Simulations of linear and nonlinear disturbances in the stratosphere," Quarterly Journal of the Royal Meteorological Society, vol. 114, no. 482, pp. 1063–1110, Jul. 1988, https://doi.org/10.1256/smsqj.48209.

[13] Nayfeh, Mahir Ali. Nonlinear dynamics in power systems. PhD diss., Virginia Tech, 1990. https://vtechworks.lib.vt.edu/server/api/core/bitstreams/311ca7dc-92fa-4d4f-8f7c-610dcc8ac981/content (Accessed on the 2nd of January 2026).

[14] L. I. Manevitch, "Complex Representation of Dynamics of Coupled Nonlinear Oscillators," Mathematical Models of Non-Linear Excitations, Transfer, Dynamics, and Control in Condensed Systems and Other Media, pp. 269–300, 1999, https://doi.org/10.1007/978-1-4615-4799-0_24.

[15] I. Andreeva and T. Efimova, "On the Qualitative Study of Phase Portraits for Some Categories of Polynomial Dynamic Systems," Cyber-Physical Systems: Modelling and Industrial Application, pp. 39–50, 2022, https://doi.org/10.1007/978-3-030-95120-7_4.

[16] F. Dercole and S. Rinaldi, "Dynamical Systems and Their Bifurcations," Advanced Methods of Biomedical Signal Processing, pp. 291–325, Apr. 2011, https://doi.org/10.1002/9781118007747.ch12.

[17] H. O. Wang, E. H. Abed, and A. M. A. Hamdan, "Bifurcations, chaos, and crises in voltage collapse of a model power system," IEEE Transactions on Circuits and Systems I: Fundamental Theory and Applications, vol. 41, no. 4, pp. 294–302, Apr. 1994, https://doi.org/10.1109/81.285684.

[18] F. Nazarimehr, S. Jafari, S. M. R. Hashemi Golpayegani, M. Perc, and J. C. Sprott, "Predicting tipping points of dynamical systems during a period-doubling route to chaos," Chaos: An Interdisciplinary Journal of Nonlinear Science, vol. 28, no. 7, Jul. 2018, https://doi.org/10.1063/1.5038801.

[19] T. Allahviranloo, "Chaos theory and chaotic systems," Decision-Making Models, pp. 465–478, 2024, https://doi.org/10.1016/b978-0-443-16147-6.00037-2.

[20] A. Sofroniou and B. Premnath, "Addressing the Primary and Subharmonic Resonances of the Swing Equation," WSEAS TRANSACTIONS ON APPLIED AND THEORETICAL MECHANICS, vol. 18, pp. 199–215, Oct. 2023, https://doi.org/10.37394/232011.2023.18.19.

[21] M. A. Laughton, "Matrix analysis of dynamic stability in synchronous multimachine systems," Proceedings of the Institution of Electrical Engineers, vol. 113, no. 2, p. 325, 1966, https://doi.org/10.1049/piee.1966.0048.

[22] S. M. Norton, T. Erdogan, and G. M. Morris, "Coupled-mode theory of resonant-grating filters," Journal of the Optical Society of America A, vol. 14, no. 3, p. 629, Mar. 1997, https://doi.org/10.1364/josaa.14.000629.

[23] P. Tielens and D. Van Hertem, "The relevance of inertia in power systems," Renewable and Sustainable Energy Reviews, vol. 55, pp. 999–1009, Mar. 2016, https://doi.org/10.1016/j.rser.2015.11.016.

[24] B. Duka and R. Duka, "On the elastic pendulum, parametric resonance and 'pumping' swings," European Journal of Physics, vol. 40, no. 2, p. 025005, Feb. 2019, https://doi.org/10.1088/1361-6404/aaf146.

[25] H. Jo and H. Yabuno, "Amplitude reduction of primary resonance of nonlinear oscillator by a dynamic vibration absorber using nonlinear coupling," Nonlinear Dynamics, vol. 55, no. 1–2, pp. 67–78, Mar. 2008, https://doi.org/10.1007/s11071-008-9345-3.

[26] Baleanu, Dumitru, Amin Jajarmi, and Jihad H. Asad. "Classical and fractional aspects of two coupled pendulums." 2019. https://rrp.nipne.ro/2019/AN71103.pdf (Accessed on the 3rd January 2026).

**Contribution of Individual Authors to the Creation of a Scientific Article (Ghostwriting Policy)**

All authors contributed to the development of this paper.

Conceptualisation, Anastasia Sofroniou; Methodology, All authors; Analytical and Numerical Analysis, Bhairavi Premnath; Validation, All authors; Writing-original draft preparation, All authors; Writing-review and editing, All authors; Supervisor, Anastasia Sofroniou.

**Sources of Funding for Research Presented in a Scientific Article or Scientific Article Itself**

No funding was received for conducting this study.

**Conflict of Interest**

The authors have no conflicts of interest to declare that are relevant to the content of this article.